

## Synthesis and Characterisation of $\text{Eu}^{3+}$ doped $\text{BaYSi}_2\text{Al}_2\text{O}_2\text{N}_5$ Nitride Based Phosphor

S. A. FARTODE<sup>1</sup>, S.J. DHOBLE<sup>2</sup>

<sup>1</sup>Department of Physics, DBA College of Engineering and Research, Nagpur-440011, India

<sup>2</sup>Department of Physics, RTM Nagpur University, Nagpur -440033, India

Email: swatifartode@gmail.com

### Abstract

Novel  $\text{Eu}^{3+}$  doped  $\text{BaYSi}_2\text{Al}_2\text{O}_2\text{N}_5$  phosphor with a general formula  $\text{Ba}_{(1-x)}\text{Eu}_x\text{YSi}_2\text{Al}_2\text{O}_2\text{N}_5$  was successfully prepared via modified two step solid state diffusion method in open air atmosphere and material were quenched at  $1200^\circ\text{C}$  for two hours.  $\text{Eu}^{3+}$  activated  $\text{BaYSi}_2\text{Al}_2\text{O}_2\text{N}_5$  phosphor was characterized by XRD, photoluminescence and FTIR techniques. The prepared phosphor was effectively excited at 394 nm, and featured intense emissions at about 592nm (orange), 614nm (red). The maximum intensity of emission was obtained for 1m% of  $\text{Eu}^{3+}$  ion. The effect of the doping concentration on the relative emission intensity of  $\text{Eu}^{3+}$  was investigated. The critical distance  $R_c$  and energy transfer mechanism for the concentration quenching of  $\text{Eu}^{3+}$  was calculated. This phosphor succeeds for Hg free excited lamp phosphor.

**Keywords:** phosphor, solid state diffusion method,  $\text{BaYSi}_2\text{Al}_2\text{O}_2\text{N}_5$ , photoluminescence.

### Introduction

The oxynitride inorganic phosphors attracted the researcher's attention owing to their potential application in solid state lighting and displays. Generally, a combination of an InGaN blue chip and a  $\text{YAG}:\text{Ce}^{3+}$  yellow-emitting phosphor is used to produce white LED [1]. However the white light produced from blue and yellow emission indicates a low color rendering index (CRI) value due to lack of red emission [2]. Hence for interior illumination it is necessary to create a high CRI value to generate warm white LEDs. For solving the deficiency two alternative approaches are currently employed using red, green and blue phosphors with a near-UV chip or using yellow and red phosphors with a blue chip [3].

Recently, the white light emitting diodes are the centre of research due to their qualities of being environmental friendly, highly efficient and having longer lifetime [4-6]. During past few years, the white-LEDs fabricated using near-UV LEDs coupled with red blue and green phosphor have attracted much attention. The current interest focuses on novel down-converting phosphors that can be effectively excited with near UV light. As far as the materials themselves are concerned; silicon oxynitride phosphors are very attractive because of their high efficiency [7,8], wide range of emission, chemical stability, good thermal quenching and ability to exhibit intense luminescence for white LEDs when activated with Eu

such as in  $Y_3Al_{5-x}Si_xO_{12-x}N_x:Ce^{3+}$  [9],  $Ba_{0.93}Eu_{0.07}Al_2O_4$  [10],  $Al_5O_6N:Ce^{3+}, Tb^{3+}$  [11],  $Y_5Si_3O_{12}N:Ce^{3+}$  [12],  $M_2Si_5N_8:Eu^{2+}$  [13–17],  $M_2Si_5N_8:Ce^{3+}$  [18],  $MSi_2O_2N_2:Eu^{2+}, Ce^{3+}$  [19–21],  $SrSi_2N_2O_2: Eu^{2+}, Ce^{3+}$  [22]  $CaSiN_2: Ce^{3+}$  [23] Ca- $\alpha$ -sialon [24]  $\beta$ -sialon [25] and  $SrYSi_4N_7$  ( $M = Sr, Ba$ ): $Eu^{2+}, Ce^{3+}$  [26]. Most prominently these phosphors emit visible light efficiently under near-ultraviolet or blue light irradiation allowing them to be used as down-conversion luminescent materials for white light-emitting diodes (LEDs). The Barium oxinitride BYN phosphor was reported by Wei-Ren Liu et al. Recent studies revealed that the research has been carried out on the luminescence properties of  $Eu^{3+}$  doped  $BaYSi_2Al_2O_2N_5$  and its corresponding application in W-LEDs. In present study the luminescence properties of  $Eu^{3+}$  doped  $BaYSi_2Al_2O_2N_5$  are reported.

### Material and method

The high temperature solid-state diffusion technique was employed for preparation of Polycrystalline  $Ba_{1-x}Eu_xYSi_2Al_2O_2N_5$  ( $0.5 \leq x \leq 2$ ) samples. High purity  $BaCO_3$  (Merck, >99.0%),  $\alpha$ - $Si_3N_4$  powder,  $Y_2O_3$ ,  $Al(NO_3)_3$  and  $Eu_2O_3$  of AR grade were the starting materials. The accurate amounts of starting materials were weighed out separately on an analytical balance and ground together in an agate mortar. The powder mixtures were fired in a furnace at  $400^\circ C$  for 1 hr. After crushing each powder mixtures for 30 mins, the powder mixtures were fired in a horizontal tube furnace (muffle furnace) at  $800^\circ C$  for 24hr in open air atmosphere. The powder mixtures were again crushed together in an agate mortar for one hour. Finally prepared materials were quenched at  $1200^\circ C$  for 2 hour rendering the powder mixture ready for further measurements.

All measurements were performed on finely ground samples that were analyzed by X-ray powder diffraction. All XRD measurements were performed at room temperature in air. The composition and phase purity of products were measured by powder X-ray diffraction (XRD) analysis with an X'Pert PRO diffractometer with Cu-K $\alpha$  radiation ( $\lambda = 1.54060 \text{ \AA}$ ) operated at 45 kV and 40 mA. The XRD data was recorded in a  $2\theta$  range from  $10^\circ$  to  $80^\circ$ . The fluorescence spectrometer (Hitachi F-4000) with spectral slit width of 1.5 nm was used to trace the photoluminescence (PL) emission spectra of the samples. The same amount of sample was used every time. Fourier transform infrared spectroscopy (FTIR) was carried out using Perkin–Elmer instrument with potassium bromide as a reference material.

### Results and discussion

**XRD Analysis:** The XRD pattern of the sample was considered for the structure confirmation. Fig. 1 represents the powder XRD pattern of  $BaYSi_2Al_2O_2N_5$  prepared by solid state diffusion technique which is in good agreement with the data reported by Wei-Ren Liu et.al [27].  $BaYSi_2Al_2O_2N_5$  crystallized as a hexagonal structure with space group of  $P6_3mc$  [27]. The reported lattice constants for  $BaYSi_2Al_2O_2N_5$  were  $a = b = 6.11862(5) \text{ \AA}$ ,  $c = 9.95227(2) \text{ \AA}$ , and the cell volume =  $322.671(6) \text{ \AA}^3$ .

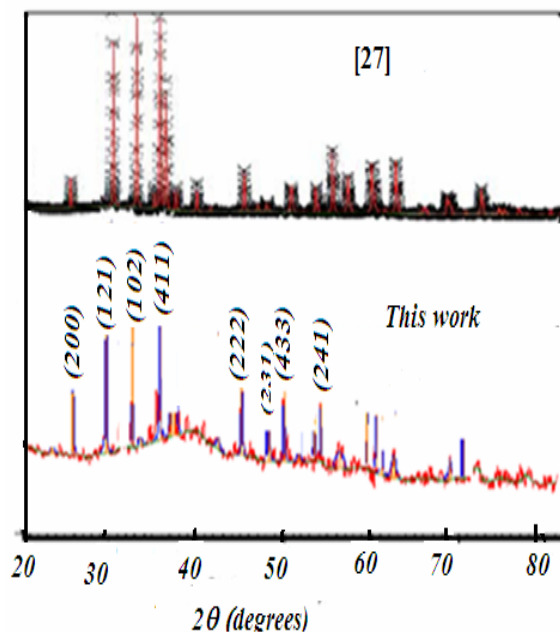


Fig.1 XRD of  $BaYSi_2Al_2O_2N_5$

One Ba atom is coordinated by twelve nitrogen atoms with three kinds of distances:  $3.07 \text{ \AA} \times 6$  (Ba-N2/O1),  $3.14 \text{ \AA} \times 3$  (Ba-N3/O3),  $2.96 \text{ \AA} \times 3$  (Ba-N3/O3) and the values for  $\alpha = 90^\circ$ ,  $\beta = 90^\circ$ ,  $\gamma = 120^\circ$ . The coordination number of  $BaYSi_2Al_2O_2N_5$  is twelve [27]. Shannon [28] reported that the ionic radii (r) of  $Eu^{3+}$  and  $Ba^{2+}$  are close to each other. So it is predicted that  $Eu^{3+}$  cation would be located in the  $Ba^{2+}$  lattice site as the  $Si^{4+}$  site are too small for  $Eu^{3+}$  to occupy.

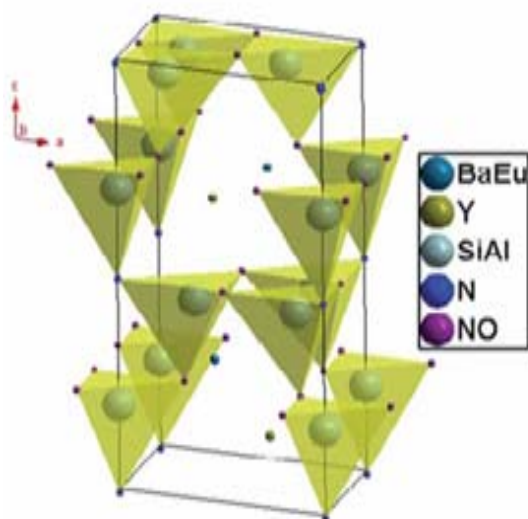


Fig.2 Crystal structure of  $BaYSi_2Al_2O_2N_5$  [27]

### Photoluminescence properties of $BaYSi_2Al_2O_2N_5 : Eu^{3+}$

Fig. 3 signifies the excitation spectrum of  $BaYSi_2Al_2O_2N_5:Eu^{3+}$  phosphors, at varied  $Eu^{3+}$  concentrations (x). The excitation spectra of  $BaYSi_2Al_2O_2N_5:Eu^{3+}$  phosphor contains peak at 394nm. The sharp peak at 394 nm is attributed to the  ${}^7F_0-{}^5L_6$  transition of doped- $Eu^{3+}$  coordinated with seven N/O

anions [29]. This excitation spectrum copes well with the emission of NUV chips, precisely required for developing NUV LED converting phosphor. Fig. 4 shows the emission spectra of BaYSi<sub>2</sub>Al<sub>2</sub>O<sub>2</sub>N<sub>5</sub>:Eu<sup>3+</sup> phosphors when excited at 394 nm at different Eu<sup>3+</sup> concentration. These samples offered intense emission peaks centered at 592 nm and 614 nm. Eu<sup>3+</sup> emission usually occurs due to <sup>5</sup>D<sub>0</sub>→<sup>7</sup>F<sub>J</sub> transitions. In general narrow emission bands may be observed at about 580, 590, 610, 650 and 700nm corresponding to transitions <sup>5</sup>D<sub>0</sub>→<sup>7</sup>F<sub>0</sub>, <sup>7</sup>F<sub>1</sub>, <sup>7</sup>F<sub>2</sub>, <sup>7</sup>F<sub>3</sub>, <sup>7</sup>F<sub>4</sub>, respectively. The transitions <sup>5</sup>D<sub>0</sub>→<sup>7</sup>F<sub>0</sub> (around 580 nm), <sup>5</sup>D<sub>0</sub>→<sup>7</sup>F<sub>1</sub> (around 590 nm) and <sup>5</sup>D<sub>0</sub>→<sup>7</sup>F<sub>2</sub> (around 610 nm) are of prime importance. The first transition is strongly forbidden transition and thus observed with appreciable intensity in some hosts. Usually, <sup>5</sup>D<sub>0</sub>-<sup>7</sup>F<sub>2</sub> is electric dipole transition whereas <sup>5</sup>D<sub>0</sub>-<sup>7</sup>F<sub>0</sub> is magnetic dipole transition. <sup>5</sup>D<sub>0</sub>→<sup>7</sup>F<sub>1</sub> is the only transition when Eu<sup>3+</sup> occupies a site coinciding with a centre of symmetry. When Eu<sup>3+</sup> ion is situated at a site which lacks the inversion symmetry, then the transitions corresponding to even values of J (except 0) are electric dipole allowed and red emission can be observed. Among all the emission peaks, the highly intense emission peak located at 593nm occurs due to the <sup>5</sup>D<sub>0</sub>-<sup>7</sup>F<sub>1</sub> transition of Eu<sup>3+</sup> and this reveals that the magnetic dipole transition is dominant in this phosphor. Further all the lines corresponding to these transitions split into number of components decided by local symmetry [30]. The crystal field splitting of both the magnetic dipole (<sup>5</sup>D<sub>0</sub>-<sup>7</sup>F<sub>1</sub>) transition and electric dipole (<sup>5</sup>D<sub>0</sub>-<sup>7</sup>F<sub>2</sub>) transition are also seen in the figure at 593 and 614 respectively.

The asymmetric ratio 'AS' is defined as the ratio of the intensity of <sup>5</sup>D<sub>0</sub>-<sup>7</sup>F<sub>2</sub> and the <sup>5</sup>D<sub>0</sub>-<sup>7</sup>F<sub>1</sub> transitions.

The asymmetric ratio is given by 
$$AS = \frac{I(614nm)}{I(593nm)}$$

where I (614 nm) and I (593 nm) is the intensity of peaks respectively at 614 and 593 nm. This ratio plays an important role to analyze any change in symmetry of Eu<sup>3+</sup> sites by giving an evaluation of degree of distortion from the inversion symmetry of the local environment of the Eu<sup>3+</sup> ion in the matrix. Therefore a large asymmetry ratio value indicates strong electric fields of low symmetry at Eu<sup>3+</sup> ions [31]. Our calculated asymmetry ratio varies from 0.9 to 1.2 for different concentration of Eu<sup>3+</sup> ion in host lattice.

The emission spectra observed at 592 nm is due to the transition from <sup>5</sup>D<sub>0</sub>→<sup>7</sup>F<sub>1</sub> and at 614 nm is due to <sup>5</sup>D<sub>0</sub>→<sup>7</sup>F<sub>2</sub>. The position of Eu<sup>3+</sup> emission line is due to interaction of M ion with Eu<sup>3+</sup> ion concentration. The energy band diagram of Eu<sup>3+</sup> is shown in Fig.5. The red emission is especially due to 4f<sup>6</sup>5d<sup>1</sup>→4f<sup>7</sup>5d<sup>0</sup> of Eu<sup>3+</sup>. The Eu ions in nitride and oxynitride compounds reduced to Eu<sup>3+</sup> due to open air ambiance. In the present compound 4f→4f emission lines begin from Eu<sup>3+</sup> in the red spectral area. It is well known that the emission band arises due to Eu<sup>2+</sup> ion whereas sharp emission line is assigned to Eu<sup>3+</sup> ion due to 4f→4f transition around 580-630 nm. [32].The stock shift of BaYSi<sub>2</sub>Al<sub>2</sub>O<sub>2</sub>N<sub>5</sub>: x%Eu<sup>3+</sup> (x =

0.2m% to 2m%) shown in table 1 was estimated to be 8303 cm<sup>-1</sup> to 8530 cm<sup>-1</sup> respectively. The emission band shifts towards longer wavelength side as the concentration of Eu<sup>3+</sup> increases. This shift can be attributed to the change in the crystal-field splitting of Eu<sup>3+</sup> [35]. This phosphor is a good member for creating white light when coupled to a blue LED chip [33].

**Table 1.** Emission wavelength and Stock Shift for BaYSi<sub>2</sub>Al<sub>2</sub>O<sub>2</sub>N<sub>5</sub>: Eu<sup>3+</sup>

Concentration	λ <sub>excitation</sub>	λ <sub>emission</sub>	Stock shift
0.2 mole%	394nm	610nm	8303 cm <sup>-1</sup>
0.5 mole%	394nm	615nm	8332 cm <sup>-1</sup>
1 mole%	394nm	618nm	8360 cm <sup>-1</sup>
2 mole%	394nm	619nm	8530 cm <sup>-1</sup>

In addition, the emission intensity of the phosphor changes as a function of doped- Eu<sup>3+</sup> content. Fig.6 shows the effect of doped-Eu<sup>3+</sup> content (x) on the emission intensity of the prepared BaYSi<sub>2</sub>Al<sub>2</sub>O<sub>2</sub>N<sub>5</sub>:Eu<sup>3+</sup> phosphor.

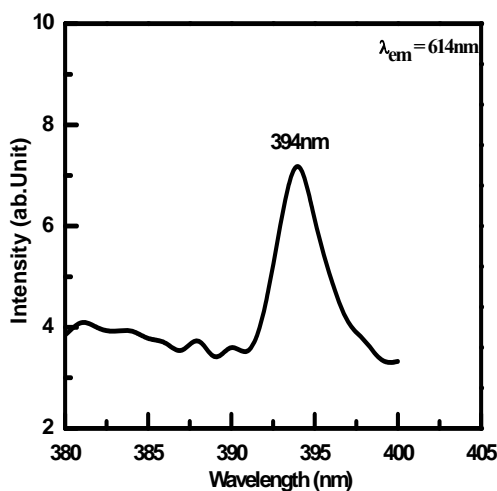


**Fig.3** Excitation spectra of BaYSi<sub>2</sub>Al<sub>2</sub>O<sub>2</sub>N<sub>5</sub>:Eu<sup>3+</sup>

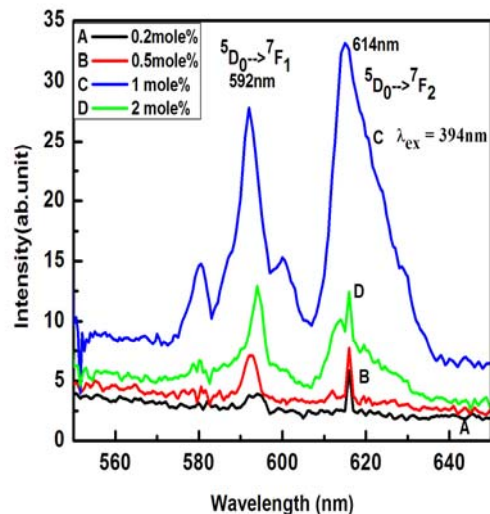


**Fig.4** Emission spectra of BaYSi<sub>2</sub>Al<sub>2</sub>O<sub>2</sub>N<sub>5</sub>:Eu<sup>3+</sup>

It can be seen that the intensity of the emission band reaches the maximum at x = 1 m% with the center locating at 614nm and decreases gradually above the critical content because of the concentration quenching effect. The concentration quenching is mainly due to energy transfer among Eu<sup>3+</sup> ions, the chances of which increases as the concentration of Eu<sup>3+</sup> increases. Wei-Ren Liu [27] Pointed out that the critical transfer distance (R<sub>c</sub>) is approximately equal to twice the radius of a sphere with the volume of the

$$\text{unit cell: } R_c = 2 \left( \frac{3V}{4\pi X_c N} \right)^{\frac{1}{3}} \quad (1)$$

where  $X_c$  is the critical concentration,  $N$  is the number of cation sites in the unit cell, and  $V$  is the volume of the unit cell. By taking the value of  $V = 322.671 \text{ \AA}^3$ , and  $X_c = 0.01$ , the critical transfer distance  $R_c$  was found to be approximately  $31.35 \text{ \AA}$ . The value of  $R_c$  was different in other  $\text{Eu}^{3+}$  doped phosphors. e.g.  $5.53 \text{ \AA}$  in  $\text{Li}_3\text{Ba}_2\text{Gd}_3(\text{MoO}_4)_8:\text{Eu}^{3+}$ ,  $8.4 \text{ \AA}$  in  $\text{Ba}_3\text{La}(\text{PO}_4)_3:\text{Eu}^{3+}$ ,  $12 \text{ \AA}$  in  $\text{Ba}_3\text{Y}(\text{PO}_4)_3:\text{Eu}^{3+}$  and  $16.7 \text{ \AA}$  in  $\text{NaCa}_4(\text{BO}_3)_3$ ,  $9 \text{ \AA}$  in  $\text{Y}_{2(1-x)}\text{Eu}_{2x}\text{MoO}_6:\text{Eu}^{3+}$ , indicating the influence of crystal structure on the luminescence of  $\text{Eu}^{3+}$  [35–39].

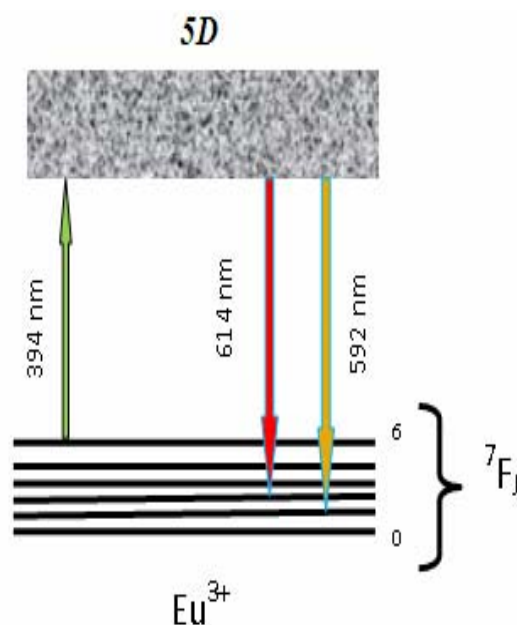


**Fig.5** Energy band diagram of  $\text{Eu}^{3+}$  in  $\text{BaYSi}_2\text{Al}_2\text{O}_2\text{N}_5$

An exchange interaction, radiation reabsorption, or electric multipolar interactions are responsible for non-radiative energy transfer from one  $\text{Eu}^{3+}$  ion to another. A large direct or indirect overlap of wave functions of donor and acceptor is requirement of the exchange interaction, and in case of forbidden transitions, exchange interaction mechanism is responsible for energy transfer. In exchange interaction the critical distance is approximately  $5 \text{ \AA}$  [34]. In the present study  $7F \rightarrow 5D$  transition of  $\text{Eu}^{3+}$  is allowed; hence, there is no role of exchange mechanism in energy transfer within  $\text{BaYSi}_2\text{Al}_2\text{O}_2\text{N}_5:\text{Eu}^{3+}$  phosphors. The mechanism of radiation reabsorption is only efficient when the fluorescence and absorption spectra are broadly overlapping. Therefore, radiation reabsorption does not occur in this case. Hence electric multipolar interaction is responsible for the process of energy transfer between  $\text{Eu}^{3+}$  ions in the  $\text{BaYSi}_2\text{Al}_2\text{O}_2\text{N}_5:\text{Eu}^{3+}$  phosphor, as suggested by Yi-Chen Chiu et al [34]. The emission intensity ( $I$ ) per activator concentration ( $x$ ) can be expressed by the following equation:

$$\frac{I}{x} = \frac{k}{1 + \beta(x)^3} \quad (2)$$

where  $k$  and  $\beta$  are constants for each type of interaction. For a given host lattice;  $\theta = 3, 6, 8, 10$  for the nearest-neighbor ions, dipole–dipole, dipole–quadrupole, quadrupole–quadrupole interactions, respectively, the above equation can be rearranged for  $\beta(x)^{\frac{\theta}{3}} > 1$  as follows [38].

After solving equation (2) become:

$$\log\left(\frac{I}{x}\right) = K' - \frac{\theta}{3} \log(x)$$

Where  $K' = \log k - \log \beta$

Fig. 7 demonstrate the variation of  $\log(I/x)$  with  $\log x$ . The  $\log(I/x)$  varies linearly with  $\log(x)$  and the slope was determined to be  $-1.74$ . The value of  $\theta$  was found to be 5.22 which is approximately equal to 6, representing that the concentration quenching mechanism of  $\text{Eu}^{3+}$  emission was governed by the dipole–dipole interaction [34].

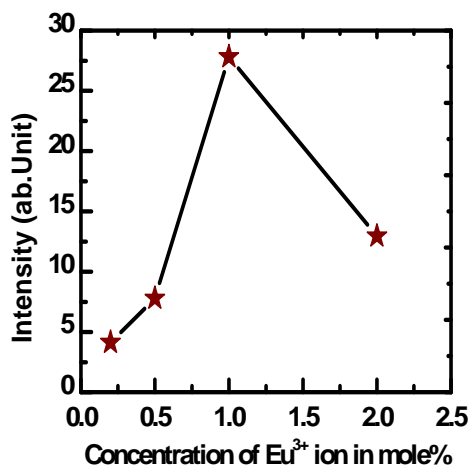


Fig.6 Variation of emission intensity with  $\text{Eu}^{3+}$  content

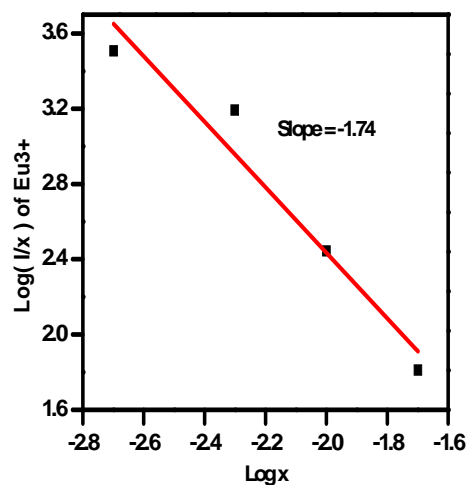
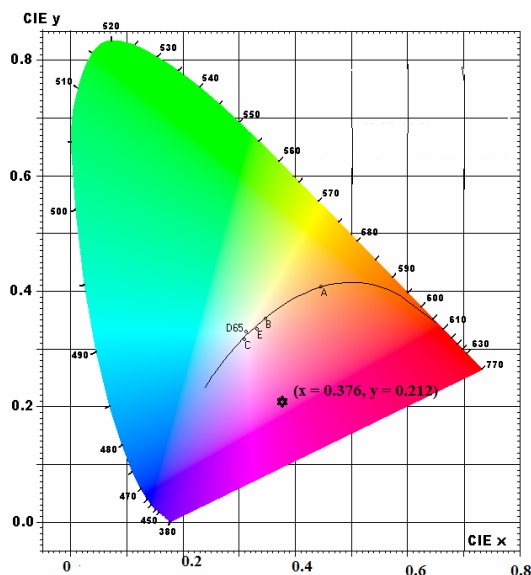


Fig.7  $\log(I/x)$  dependence of  $\log(x)$

### Chromatic properties of $\text{Eu}^{2+}$ doped $\text{BaYSi}_2\text{Al}_2\text{O}_2\text{N}_5$ :

As per the 1931 Commission Internationale de l'Eclairage (CIE) chromatic color coordinates refer to the largest part lighting stipulations. Red, green and blue are three primary colors which identifies the chromatic color coordinates.



**Fig. 8** CIE color coordinates

These colors are employed by human visual system. . In general, (x, y) coordinate represents the color of several light sources in the color space. The color purity was evaluated with the 1931 CIE Standard Source C (illuminant Cs (0.3101, 0.3162)) [40]. The location of the color coordinates of the BaYSi<sub>2</sub>Al<sub>2</sub>O<sub>2</sub>N<sub>5</sub>: Eu<sup>3+</sup> nitride phosphor and the CIE chromaticity diagram showed in Fig.8. The coordinates for the phosphor are (x = 0.376, y = 0.212) shown by star.

### FTIR Study:

The bonding of atoms to each other or grouping of atoms in a molecule was studied by IR spectroscopy. Infrared spectroscopy is used to study the vibrational motions of molecules. The changes in the vibrational energy of the molecules arise due to absorption of energy in the infrared region. There are two types of vibrations that cause absorptions in an IR spectrum. The alternate increase and decrease in interatomic distance or rhythmic displacement along the bond axis arises in stretching vibrations and a change in bond angles between two bonds in an atom occurs in bending vibrations [42]. The IR spectra of the samples in the wave number range from 4000 to 400 cm<sup>-1</sup> as a function of percentage transmittance is made known in Fig. 9.

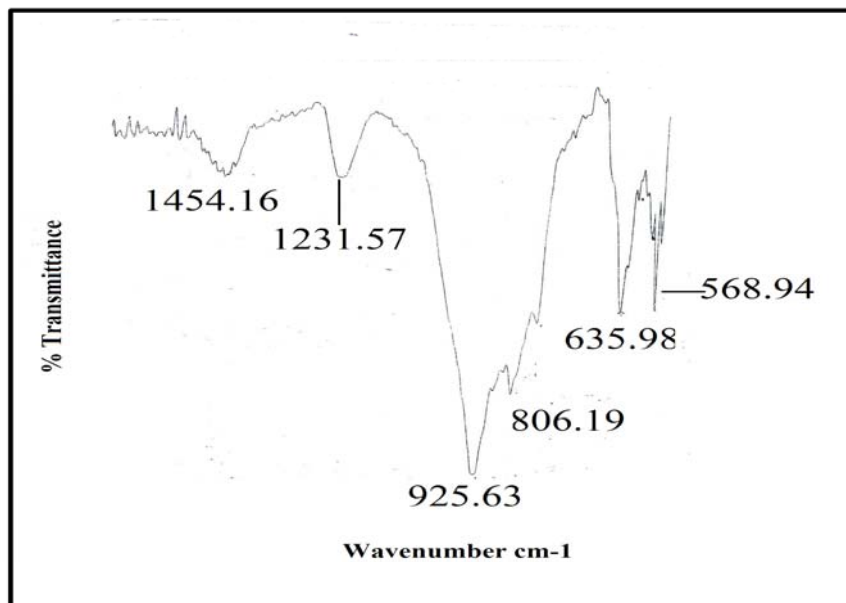


Fig.9.FTIR spectra of BaYSi<sub>2</sub>Al<sub>2</sub>O<sub>2</sub>N<sub>5</sub>phosphor

The IR spectrum of the samples has absorption band at 1454.16 and 1433.50 cm<sup>-1</sup> which could be allocated to the weak bending of N=O bonds [42] and the absorption band at 1213.57 cm<sup>-1</sup> could be due to weak stretching of N-O bond [42]. The broad and strong absorption bands with multiple peaks below 1000 cm<sup>-1</sup> are attributed to resonance of metal oxygen bands [39]. The band observed at 925.63 cm<sup>-1</sup> is due to Si-O(N) bending [41]. The bands at 568.94, 635.98, 806.19 cm<sup>-1</sup> are assigned to bending of Y-O, stretching of M-NO<sub>2</sub> (M=metal atom) and symmetric stretching of Si-O-Si [41,42]. The new absorption peaks located at 578.21, 559.49, and 856.29 cm<sup>-1</sup> may be due to some impurity phases.

## Conclusion

In the present work the samples were prepared by high temperature modified two step solid state diffusion method. The luminescence properties of Eu<sup>3+</sup> in BaYSi<sub>2</sub>Al<sub>2</sub>O<sub>2</sub>N<sub>5</sub> material were investigated. It shows the visible emission band peaking at 592nm and 614nm under near UV excitation 394nm for Eu<sup>3+</sup>. The series of BaYSi<sub>2</sub>Al<sub>2</sub>O<sub>2</sub>N<sub>5</sub>:Eu<sup>3+</sup> phosphors with various concentrations of dopant (0.2 Mole % to 2 Mole %) were prepared and the effect of doping concentration on the emission intensity of BaYSi<sub>2</sub>Al<sub>2</sub>O<sub>2</sub>N<sub>5</sub> was investigated. The emission intensities of phosphor vary with dopant concentration. The color coordinates were found to be (x ≈ 0.376, y ≈ 0.212). The variation of log(x) with log(I/x) was found to be linear indicating that the concentration quenching mechanism of Eu<sup>3+</sup> emission was controlled by dipole-dipole interaction.

## References

- [1] Nakamura S., Seno M., Mukai T. //Appl. Phys Lett. V.62, P.1687-1689,1994
- [2] Kim J.U., Kim Y.S., Yang H.S.// Mater. Lett. V.63,P.614-616,2009.

- [3] Kim D.H., Ryu J.H., Cho S.Y.//Appl. Phys A V.102,P.79-83,2011.
- [4] Im W.B., Kim Y.I., Fellows N.N., Masui H., Hirata G.A., Denbaars S.P.,Seshadri R.// Appl.Phys.Lett.V.93,P.091905(1-3),2008.
- [5]Nishida T., Ban T., Kobayashi N.//Appl.Phys.Lett. V.82, P.3817-3819,2003.
- [6] Kim J.S., Jeon P.E., Choi J.C., Park H.L., Mho S.I., Kim G.C. //Appl.Phys.Lett.V.84,P.2931-2933,2004.
- [7] Duan C.J., Otten W.M., Delsing A.C.A., Hintzen H.T. //J Alloys and Compds V.461,P.454-458,2008.
- [8] Suehiro T., Hirosaki N., Xie R.J., Sakuma K., Mitomo M., Ibukiyama M., Yamada S.//Appl. Phys. Lett. V.92 ,P.191904 (1-3),2008.
- [9] Chung J.H., Ryu J. H. //J Ceramics International.V.38 ,P.4601-4606,2012.
- [10] Li X., Budai J. D, Liu F., Howe J. Y. , Zhang J., Wang X.J. , Gu Z., Chengjun S., Meltzer R. S., Pan Z. // J Light: Science & Applications V.2(2013), P.e50-(1-8),2008.
- [11] Hu W.W., Zhu Q.Q., Hao L.Y., Xu X.,Agathopoulos S.// J Lumin.V.149, P. 155-158,2014.
- [12] Lu F.C., Guo S.Q., Yang Z.P., Yang Y.M., Li P.L. Liu Q.L. // J Alloys and Compds V. 521,P.77-82, 2012.
- [13] Hoppe H.A., Lutz H., Morys P., Schnick W., Seilmeier A. // J Phys. Chem. Solids V. 61(12), P. 2001-2006, 2000.
- [14] Smet P.F., Adrie K.V.D.E., Bos J.J., Kolk E.V., Dorenbos P.// J Lumin. V. 132, P. 682-689, 2012.
- [15] Li Y.Q., van Steen J.E.J., Krevel J.W.H.V., Botty G., Delsing A.C.A., DiSalvo F.J.,With G.De, Hintzen H.T. // J Alloys Compd. V.417, P. 273-279,2006.
- [16] Xie R.J., Hirosaki N., Suehiro T., Xu F.F., Mitomo M. // Chem. Mater.V.18, P.5578- 5583, 2006.
- [17] Piao X.Q., Horikawa T., Hanzawa H., Machida K. // Appl. Phys. Lett.V. 88, P.161908(1-3), 2006.
- [18] Li Y.Q., With G. De, Hintzen H.T. // J Lumin. V.116, P.107-116,2006.
- [19] Li Y.Q., With G. De, Hintzen H.T. // J Mater. Chem. V.15,P. 4492-4496,2005.
- [20] Zhang Z.J., Kate O.M.T., Delsing A, Dorenbos P., Zhao J.T., Hintzen H.T. // J Mater. Chem. C V. 2 P. 7952-7955,2014.
- [21] Bachmann V., Jüstel T., Meijerink A., Ronda C., Schmidt P.J. // J Lumin.V.121, P.441-449,2006
- [22] Li Y. Q., Delsing A. C. A., With G. De, Hintzen H. T. // Chem. Mater V.17, P. 3242-3248, 2005.



- [23] Toquin R. Le, Cheetham A.K. //Chem. Phys. Lett. V.423,P. 354-356, 2006.
- [24] Suehiro T., Hirosaki N., Xie R.J. Mitomo M. // Chem. Mater V.17, P.308-314, 2005.
- [25] Hirosaki N., Xie R.J., Kimoto K., Sekiguchi T., Yamamoto Y., Suehiro T. Mitomo M./Appl. Phys. Lett. V.86, P.211905 (1-3),2005.
- [26] Li Y.Q., Fang C.M., With G. de, Hintzen H.T. // J Solid State Chemistry, V.177, P.4687-4694,2004.
- [27]Liu W.R, Yeh C.W., Huang C.H., Lin C. C., Chiu Y.C., Yeh Y.T., Liu R.S. // J Mater. Chem. V.21, P. 3740-3744,2011
- [28] Shannon R. D., Acta Crystallogr. V.A 32(5), P. 751-767, 1976.
- [29] Blasse G., Phil B.A. // Tech. Rev. V.31 (10), P. 304-306, 1970.
- [30] Kumar M., Seshagiri T.K., Godbole S.V. // Physica B V.410, P. 141-146, 2013.
- [31] Xie R.J., Hirosaki N., Mitomo M., Yamamoto Y., Suehiro T., Sakuma K. // J. Phys. Chem.B V. 108(32), P. 12027-12031,2004.
- [32] Li Y.Q., Ph.D thesis 2005,Eindhoven university of Technology, Eindhoven, The Netherlands.
- [33] Zhang Y.Q., Liu X.J. , Huang Z.R. , Chen J., Yang Y.// J Lumin.V.132,P. 2561-2565,2012.
- [34] Chiu Y.C., Huang C.H., Lee T.J., Liu W.R., Yeh Y.T., Jang S.M., Liu R.S. // Optics Express V.19, P. A331-A339, 2011.
- [35] Chang Y.C., Liang C.H., Yan S.A., Chang Y.S. //J Phys. Chem. C V.114, P. 3645-3652, 2010.
- [36] Yu R.J., Noh H.M., Moon B.K., Choi B.C., Jeong J.H., Jang K., Yi S.S., Jang J.K. // J Alloys Compd.V. 576, P. 236-241,2013.
- [37] Xin S.Y., Wang Y.H., Wang Z.F., Zhang F., Wen Y., Zhu G. //Electrochem. Solid State Lett. V. 14, P. H438-H441, 2011.
- [38] Zhang X.M., Seo H.J. // J Alloys Compds. V.503, P. L14-L17, 2010.
- [39] Han B., Zhang J., Wang Z., Liu Y., Shin H. // J Lumin. V.149, P. 150-154, 2014.
- [40] Kohale R.L., Dhoble S.J.// Micro & Nano Lett.V.7,P. 453-455,2012.
- [41] Geng D., Lian H., Shang M., Zhang Y., Lin J. // Inorg.Chem. V. 53, P. 2230-2239, 2014.
- [42] Cooke J. 2005, Department of Chemistry, University of Alberta,